Fibre Bragg Grating Based Continuous-Phase Encoder-Decoders for OCDMA Networks

Zhaowei Zhang, Chun Tian, Periklis Petropoulos, David J. Richardson and Morten Ibsen
Optoelectronics Research Centre, University of Southampton, Southampton, SO17 1BJ, UK zhz@orc.soton.ac.uk

Abstract *Continuous-phase OCDMA encoder-decoders are proposed and demonstrated. Compared with conventional discrete-phase devices, they have additional advantages of being more tolerant to input pulse-width and furthermore will facilitate the use of reconfigurable phase-codes.*

Introduction

Optical CDMA (OCDMA) systems based on temporal-phase-encoding using super-structured fibre Bragg gratings (SSFBGs) has been demonstrated as a promising technique for future optical networks [1]-[3] where the SSFBG encoder-decoders have a spatial phase distribution following a particular address code. In the encoding process, the optical pulses are reflected from the SSFBG encoder, and the spatial phase of the encoder is encrypted into the temporal phase of the encoded pulse. For successful decoding, the encoded pulses must be reflected from an SSFBG decoder of the conjugate address code to the encoder. To enhance the flexibility of this approach we recently demonstrated a reconfigurable FBG en/decoder, in which the phase shifts are produced by a thermally induced background refractive index variation, which are inherently of a continuous nature [4].

In this work, we propose and demonstrate a novel fixed phase-en/decoder with a continuous-phase profile designed to match a reconfigurable en/decoder. We find that it exhibits similar performance to a fixed discrete-phase en/decoder and additionally can accommodate longer input pulse widths compared to these.

Device description

For the discrete-phase en/decoders mentioned above, a spatial gap ΔL in the grating structure constitutes a phase-shift $\phi = \frac{4\pi}{\lambda_B} n_{eff} \Delta L$. While for the continuous-phase en/decoders, the phase-shift is given by $\phi = \frac{4\pi}{\lambda_B} \int \delta n_{eff}(x) dx$, where $\delta n_{eff}(x)$ is the additional effective refractive index change [4].

Two 16-bit quaternary codes Q1 and Q2 are chosen from the family *A* sequences [2] [5]. Q1C and Q2C denote the *continuous-phase*-encoders, whilst Q1D and Q2D represent the *discrete-phase*-encoders. Q1C*, Q2C*, Q1D* and Q2D* are corresponding decoders. The chip length of them is 2.5mm.

For Q1C and Q2C, the effective refractive index distributions corresponding to a single phase-shift 0.5π, 1.0π and 1.5π are shown in Fig.1 (a). Note that this distribution is the same as the thermally induced phase-shift-distribution in the reconfigurable encoder reported in [4]. The effective refractive index distribution of Q1C is shown in Fig.1(b) as an example. For comparison, the phase profile of Q1D is shown in Fig.1(c). Note that Q1D and Q1C have identical phase code sequences.

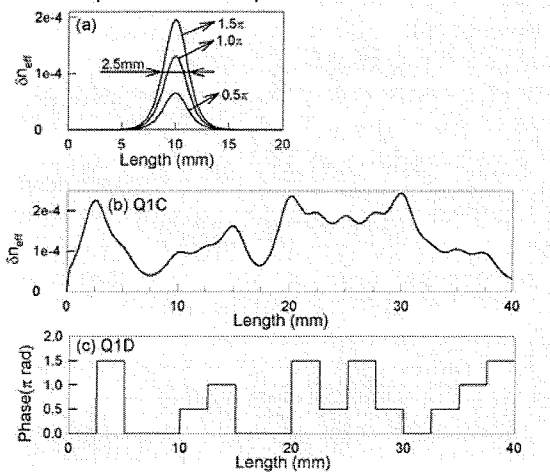

Fig.1 Effective refractive index distributions of (a) a single phase-shift and (b) continuous-phase encoder Q1C (c) The phase of discrete-phase encoder Q1D

Device fabrication and characterization

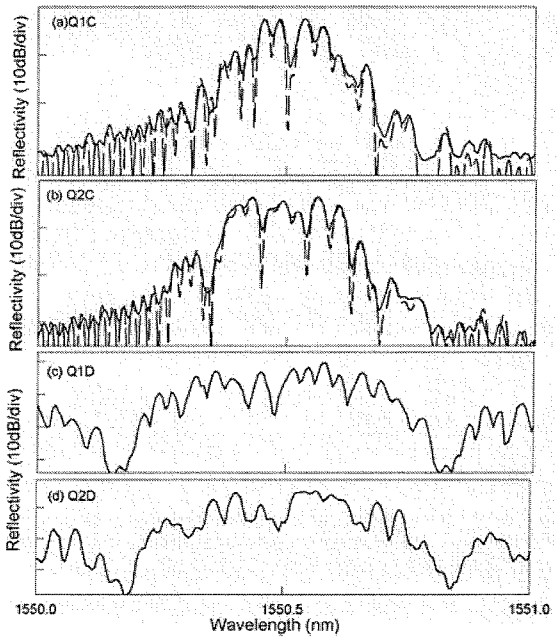

Fig.2 Measured (solid lines) and simulated (dashed lines) reflection spectra of continuous-phase encoders (a) Q1C, (b) Q2C, discrete-phase encoders (c) Q1D and (d)Q2D.

All the en/decoders are fabricated using our continuous grating writing technique [6], which uses a phase mask with uniform pitch and relies on precise control of the position of the fibre relative to phase mask to achieve gratings with complex profiles. The effective refractive index variation, δn_{eff}, in the continuous-phase en/decoders is achieved by chirping the Bragg wavelength, $\delta\lambda_B$, (according to the equation $\delta n_{eff} = \frac{\delta\lambda_B}{\lambda_B} n_{eff}$). For comparison, we also fabricate discrete-phase en/decoders. The Bragg wavelength, index modulation, chip length, and total length of all the gratings are respectively 1550.5nm, 2.2×10^{-5}, 2.5mm and 40mm.

Fig. 2 (a) and (b) shows the simulated and measured reflection spectra of the continuous-phase-encoders Q1C and Q2C. There is clearly good agreement between the measurement and simulation results. Shown in Fig. 2(c) and (d) are the measured reflection spectra of discrete-phase-encoders Q1D and Q2D. Note that for the same nominal address codes, the reflection spectra of the continuous-phase-encoders are narrower than those of the discrete-phase-encoders and that they have much lower spectral features away from the main band, which could assist their use in a WDM configuration.

Device performance and discussion

The codes are all tested using a gain-switched laser diode, operating at 1550.5 nm, and generating ~5 ps pulse sequences with a repetition rate of 311 MHz. This pulse train is split by a 3dB coupler into two parts, each reflected from the continuous-phase encoders Q1C and Q2C respectively, and then combined by another 3dB coupler. A fibre delay line controls the timing of the signals from the two encoding gratings. Then the combined signal is reflected from the continuous-phase decoders Q1C* or Q2C*.

The decoded pulses are detected using a 20GHz photodiode and fed into a fast sampling oscilloscope. The measured auto- and cross correlation pulses, for the decoders Q1C* or Q2C*, are shown in Fig. 3(a). The measured ratio between the peak of the cross and auto correlation (RPCA) is ~20%. For comparison, we also measure the system using the discrete-phase encoders (Q1D, Q2D) and decoders (Q1D*, Q2D*), (Fig.3(b)). In this case, the measured RPCA is also ~ 20%.

For further comparison, the performances of systems using continuous-phase or discrete-phase devices with the same chip duration and code sequences are simulated under different input pulse-widths. The resultant RPCA is summarized in Fig.4. We can see that the system using the continuous-phase en/decoders are more tolerant to longer input pulse-widths. This we believe can be explained by the fact that the reflection spectrum of the continuous-phase device is narrower than that of the discrete-phase device, as shown in Fig. 2.

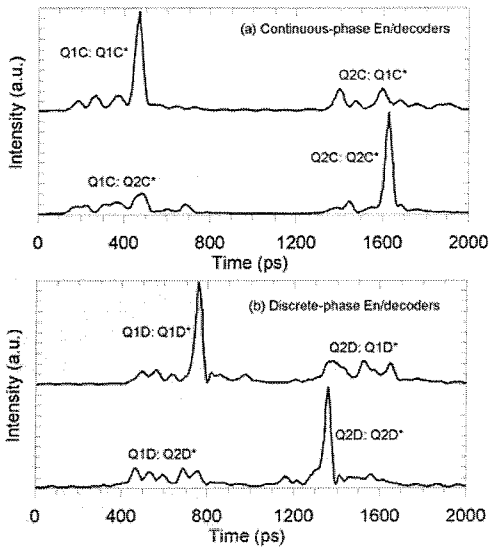

Fig. 3 Measured decoded pulses for systems using (a) continuous-phase and (b) discrete-phase en/decoders.

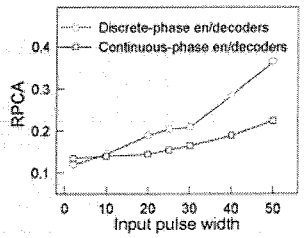

Fig. 4 Simulated RPCA for systems using continuous or discrete-phase en/decoders for different input pulse widths.

Conclusions

We have demonstrated a new OCDMA phase en/decoder based on FBGs. Its performance is compared with a system using the discrete-phase devices. The advantage of the new continuous-phase devices includes that it has a more relaxed requirement on the encoding input pulse width. This suggests the potential of bandwidth saving, and could facilitate the combination of an OCDMA system with existing WDM techniques to enhance system capacity further. The new code design will also facilitate a better match to reconfigurable en/decoders, because they have same spatial phase distributions [4].

References

1 P. C. Teh et al, Journal of Lightwave Technology, 19(2001), pp.1352-1365.

2 P. C. Teh et al, IEEE Photonics Technology Letters, 14(2002), pp.227-229.

3 X. Wang et al, in proceedings to *OFC2005*, PDP33.

4 Z. Zhang et al, in proceedings to *OFC2006*, OFF1.

5 S. Boztas et al, IEEE Transactions on Information Theory, 38(1992), pp.1101-1113.

6 M. Ibsen et al, IEEE Photonics Technology Letters, 10(1998), pp.842-844.